PHILOSOPHICAL TRANSACTIONS OF THE ROYAL SOCIETY A
MATHEMATICAL, PHYSICAL & ENGINEERING SCIENCES

Earth's Plasma Environment: Magnetic Reconnection and Its Effect on Magnetospheric Fields and Flows

S. W. H. Cowley

Phil. Trans. R. Soc. Lond. A 1994 **349**, 237-247
doi: 10.1098/rsta.1994.0128

Earth's plasma environment: magnetic reconnection and its effect on magnetospheric fields and flows

By S. W. H. Cowley

Blackett Laboratory, Imperial College of Science, Medicine and Technology, London SW7 2BZ, U.K.

Spacecraft observations of the Earth's magnetosphere have revealed the presence of a complex spatially structured plasma and field environment, which undergoes significant variations on time-scales from minutes to years. Magnetospheric plasma originates in the solar wind and the ionosphere, and the principal transport process is a twin-vortical flow driven by coupling to the solar wind. We review present understanding of the coupling process and some consequences which follow.

1. Introduction

Investigation of the Earth's ionized environment began 35 years ago when *in situ* measurements of particles and fields became available from spacecraft. A vast amount of information has now been collected, which, although deficient in some critical areas, has revealed a complex structured and dynamic plasma system, outlined in figure 1. Magnetospheric plasma originates in the solar wind and the ionosphere (Cowley 1993). The solar wind is a source of warm (several hundred eV) proton and alpha particle (He^{2+}) plasma, while the ionosphere is a source of cold (several eV) proton and singly-charged helium (He^{+}) plasma, though intense streams of accelerated ions (10 eV–10 keV), including oxygen (O^{+}), flow out of the auroral zone ionosphere. Observations of the plasma flow have also revealed that the principal transport process is a twin-vortical convective flow driven by coupling to the solar wind. The nature of the coupling has been much debated, though now largely settled as follows. Although several processes may contribute (e.g. Kelvin–Helmholtz waves at the boundary, or wave-driven spatial diffusion of plasma), by far the most significant is electromagnetic in nature and depends upon the local direction of the interplanetary magnetic field (IMF), namely magnetic reconnection first proposed in a magnetospheric context by Dungey (1961). Here we first review evidence for the occurrence of reconnection at the magnetopause, and then look at two unique consequences, namely partial penetration of the IMF into the magnetosphere, and the modulation of the interior flow according to the IMF direction.

Phil. Trans. R. Soc. Lond. A (1994) **349**, 237–247
Printed in Great Britain

TEX Paper

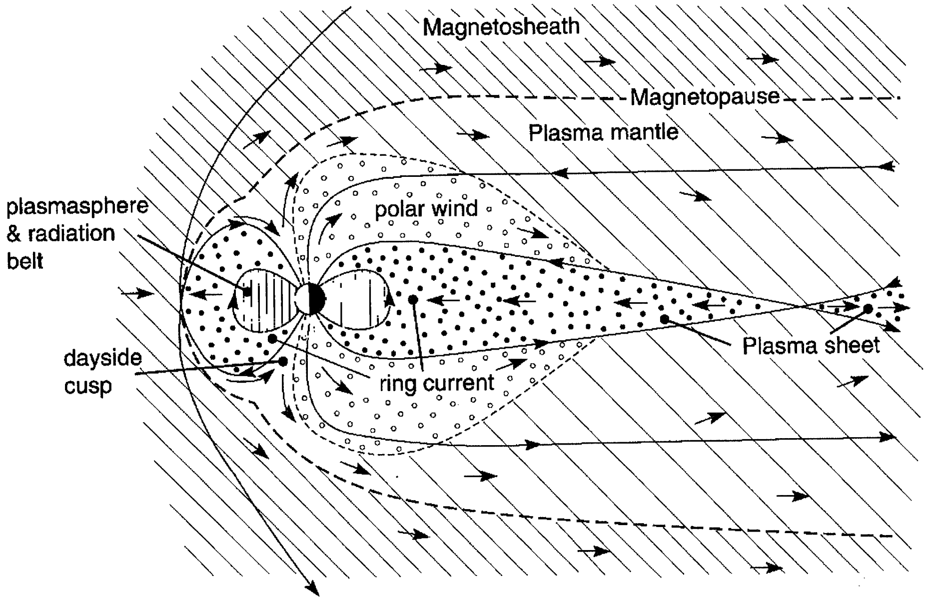

Figure 1. The principal features of the Earth's magnetospheric field (solid lines) and plasma populations.

2. Dayside magnetopause reconnection

Reconnection between the magnetosheath and magnetospheric fields at the low-latitude magnetopause is a consequence of field diffusion relative to the plasma within the current sheet, and results in the formation of 'open' field lines which cross the boundary (Cowley 1985). The most important consequence is that the open tubes provide a means of transferring solar wind momentum into the magnetosphere via magnetic stresses; the open tubes are swept from the dayside to the nightside by the solar wind and stretched into a magnetic tail. Locally, however, the occurrence of reconnection can be recognized by two other effects, the mixing of magnetosheath and magnetosphere plasmas along the open tubes, and the acceleration of those populations by the field when they flow into the current sheet. The initially highly distended open tubes contract away from the site of reconnection under the action of magnetic tension at the Alfvén speed V_{A} (corresponding to the inflow plasma), and the ions which move into the sheet are accelerated as though they were hit by a mirror moving at that speed (Cowley 1982). Consequently the accelerated ions form a field-aligned beam streaming out along the open tubes at $\sim 2V_{\mathrm{A}}$ (independent of ion species if they are all of low initial bulk speed), directed away from the reconnection site on either side. If the current sheet thickness is comparable with the ion gyroradius (or less), i.e. $\sim$ 100 km, as some observations suggest, then the ion motion within the layer will be non-adiabatic and the accelerated ions can emerge on either side of the layer. That is, these ions can either be reflected from the current sheet or transmitted, forming a wedge-shaped accelerated boundary layer of mixed origins on both sides of the boundary.

The expected form of the inflow and outflow ion distributions are shown in figure 2, simplified from Cowley (1982). We assume for simplicity that the mag-

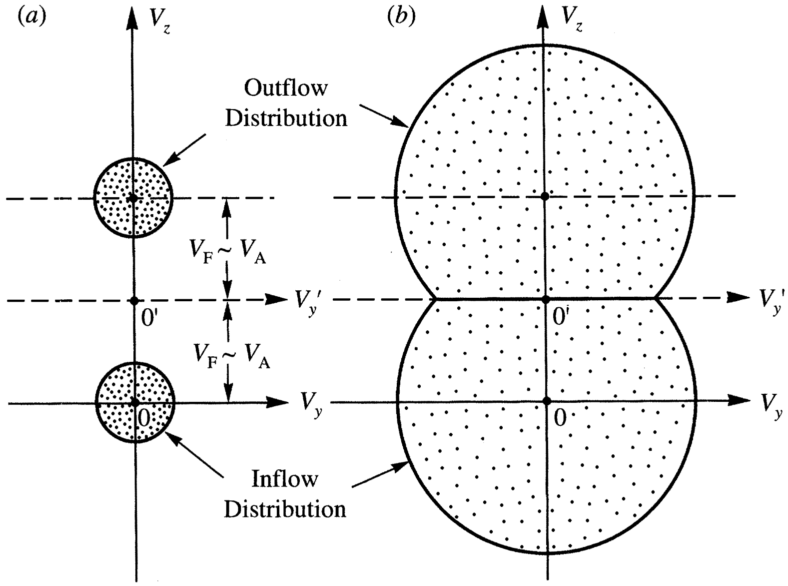

Figure 2. The form of the inflow and outflow ion velocity distributions for reconnection-associated magnetopause current sheet acceleration, for the case of (a) cold and (b) hot ion populations.

netospheric field is directed to the north ($+Z$) and the magnetosheath field to the south ($-Z$) but are of similar magnitude (typically several tens of nT), and that the field component threading the current sheet (X-direction) is much smaller than either (typically a few nT). Figure 2a shows the case of a population whose thermal speed is much less than the field line speed, e.g. ionospheric plasma whose thermal speed is a few tens of km s^{-1} compared with field line speeds ($\sim V_A$) of a few hundred. The plane of the diagram is that of the magnetopause, with V_z along the field directions outside the current sheet, and V_y in the direction of the current; the dotted circles represent projections of the ion distribution onto this plane. The incident ions are assumed to have zero bulk flow in the Earth's frame (apart from a small $\boldsymbol{E} \times \boldsymbol{B}$ drift into the current sheet in the X-direction) and is hence centred on O, the origin of velocity space in the Earth's frame. Assuming a location north of the reconnection site, O′, located at speed $\sim V_A$ along the V_z-axis, is then the origin in the field line (de Hoffman–Teller) frame, and the outflow distribution is just a mirror reflection of the inflow distribution about the V_y'-axis. It thus forms a beam moving northwards along the reconnected field lines at speed $2V_A$. Scattering within the current sheet will tend to spread the outflow distribution over spherical shells centred on O′.

Figure 2b shows the case of a hot ion component whose thermal speed is comparable with or larger than the field line speed, e.g. magnetosheath ions with thermal speeds of a few hundred km s^{-1} and magnetospheric ring current ions with thermal speeds of order a thousand km s^{-1}. In this case the inflow distribution is truncated to V_z values lower than the field line speed (the region below O′), since ions with a larger V_z escape without interacting with the current sheet. The outflow distribution is again a mirror image in the V_y'-axis (in the absence of scattering in the current sheet), and hence is again centred on $V_z = 2V_A$ (if the inflow bulk speed is zero), but truncated at speeds below the field line speed. The outflow distribution thus has a characteristic D-shape, with a cut-off at the Alfvén speed. This applies strictly only at the surface of the current sheet. On moving away from the surface the interface between the two populations moves along the V_z-axis to larger speeds, reaching infinity at the field separatrix mapping to the reconnection site.

Experimental verification of these predictions is not simple. The reconnection rate often appears to be pulsed rather than steady as assumed above, leading to characteristic ~ 2 minute field perturbations termed 'flux transfer events' (FTEs) (Russell & Elphic 1979). Even when the reconnection rate is more steady, the boundary is often in rapid motion (several tens of km s^{-1}) such that boundary layers of ~ 1000 km thicknesses are swept across spacecraft in a few tens of seconds. Particle observations with good time, velocity space, mass and charge state resolution are thus required to address this problem in detail. The earliest observations which approached the required characteristics were obtained by the ISEE-1 and ISEE-2 spacecraft, and for a few well-studied examples the field and plasma data were successfully compared with predictions based on magnetohydrodynamic considerations at a one-dimensional current layer (Sonnerup *et al.* 1981).

The first comparisons at a kinetic level by Smith & Rodgers (1991) used AMPTE-UKS data, and showed that the accelerated magnetosheath population was indeed of D-shaped form with a cut-off at the field line speed. A further dimension was added by observations with mass and charge-state resolution obtained by AMPTE-CCE, as shown in figure 3 (Fuselier *et al.* 1991). This shows contours of the ion velocity distribution in the plane of the magnetopause, as in figure 2, together with cuts through the ion distribution along the field direction. Results are shown for an interval inside the magnetosphere (A), in the magnetospheric boundary layer (B), the magnetosheath boundary layer (C) and magnetosheath proper (D). Data are shown for ionospheric He^+ and solar He^{2+}. Panel A shows He^+ which is peaked perpendicular to the magnetic field (arrow labelled B). The left side of panel B shows the He^+ distribution in the magnetospheric boundary layer. This consists of two components, a low-V_z inflow component (which has nevertheless been heated compared with A (note the scale change between A and B) and has acquired a large field-perpendicular flow in the $-V_y$-direction), and a second component which is further heated and moving northwards along the field with a speed $2V_A$ relative to the first. This represents He^+ ions accelerated (and somewhat scattered) in the current sheet and reflected back into the magnetosphere. The field line speed is given by the black dot along the $\boldsymbol{B}$-direction which bisects the two distributions. The He^{2+} distribution shown on the right of panel B is dominated by transmitted magnetosheath ions, and correspondingly shows a D-shaped distribution with a cut-off at the field line speed. There is also a weak cold ionospheric He^{2+} component which has the same velocity as the inflow He^+, but any reflected component is lost within the body of the transmitted magnetosheath population. The He^+ distribution in the magnetosheath boundary layer (C, right) is a transmitted magnetospheric component, accelerated along the field to $\sim 2V_A$, but also considerably spread in velocity space. Finally, He^{2+} in the magnetosheath boundary layer (C, left) consists of a central 'core' of inflowing ions (compare with the undisturbed He^{2+} distribution in panel D), together with an accelerated scattered reflected component flowing antiparallel to the field with speeds above the field line speed. These data pro-

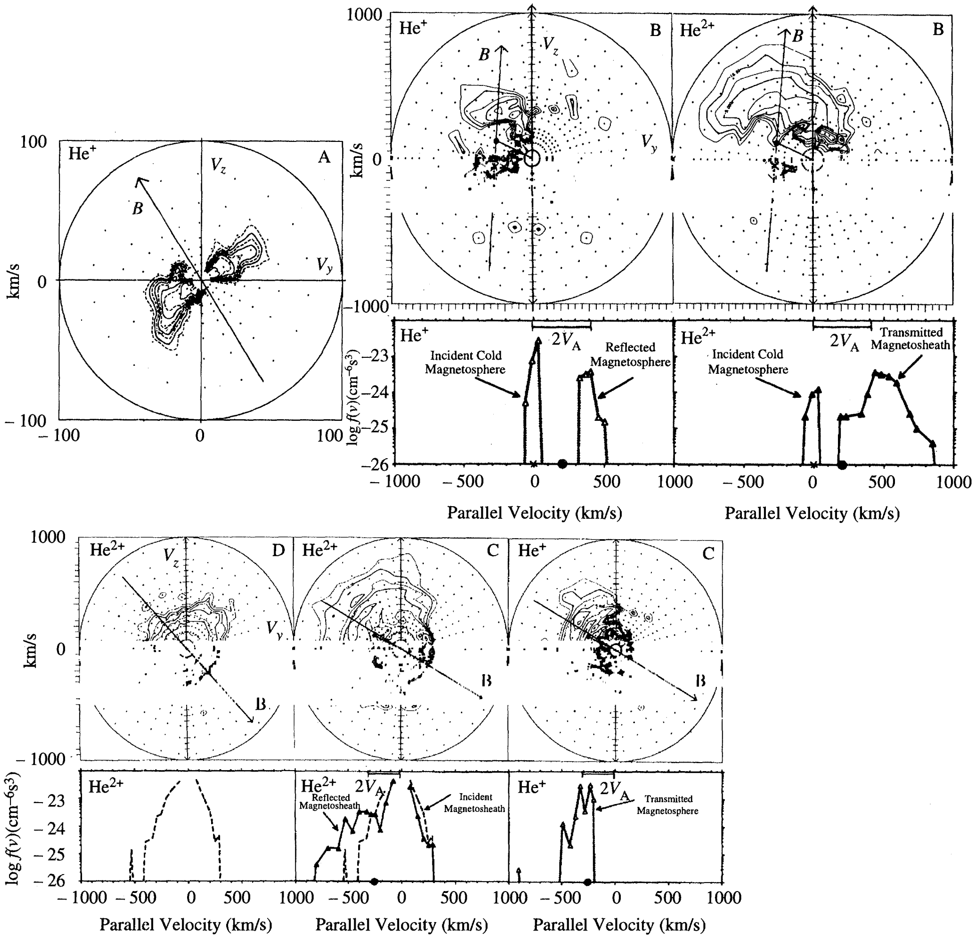

Figure 3. AMPTE-CCE observations of He^+ and He^{2+} distributions in the magnetosphere (panel A), magnetospheric boundary layer (B), magnetosheath boundary layer (C) and magnetosheath (D). (From Fuselier *et al.* (1991).)

vide striking confirmation of theoretical expectations, and serve to illustrate the way in which detailed analysis of high-quality data can be used to study specific plasma kinetic processes in space.

3. IMF penetration into the magnetosphere

A consequence which is unique to reconnection coupling at the magnetopause is a partial penetration of the IMF into the magnetosphere. The general principle behind this effect (D. J. Southwood, personal communication 1981) is that following reconnection the system tends to relax under the action of magnetic stresses toward a state of reduced stress. The state of zero electromagnetic stress

PHILOSOPHICAL TRANSACTIONS OF THE ROYAL SOCIETY A MATHEMATICAL, PHYSICAL & ENGINEERING SCIENCES

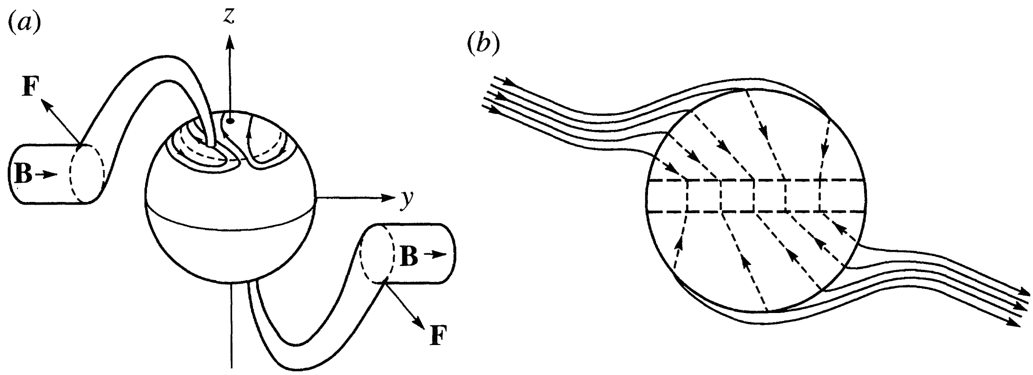

Figure 4. The effect of IMF B_y on the evolution of open tubes (*a*) on the dayside and (*b*) in the tail.

corresponds to a linear superposition of the Earth's field and the IMF, though this is never fully achieved.

Figure 4 shows how this works for the Y-component of the IMF (Cowley 1981). Figure 4*a* is a view of the dayside of the Earth, and shows newly opened flux tubes in the presence of positive B_y. The magnetic tension pulls the tubes to the west in the northern hemisphere and to the east in the southern hemisphere, producing corresponding oppositely directed flows in the ionosphere, together with a range of other asymmetries (Cowley *et al.* 1991). The consequence is that open tubes are added preferentially to the dawn side of the northern tail lobe and to the dusk side of the southern lobe.

Figure 4*b* shows a cross-section through the tail where the open flux enters the tail preferentially on the dawn side of the northern lobe and exits preferentially on the dusk side of the southern lobe. Flux conservation then requires a net flux across the tail in the direction of IMF B_y, in accordance with the general principle. However, the interior field will be smaller than the IMF because only a fraction of the IMF which is brought up to the magnetosphere becomes attached. Most is diverted around the sides of the magnetosphere as expected for perfectly conducting flow around a blunt obstacle. This is indicated in figure 4 by showing that the open flux maps into a narrow slice of the undisturbed IMF away from the cavity. The fraction of the IMF which appears inside is roughly the same as the fraction of the impinging IMF which becomes connected, which is the same as the ratio of the voltage imposed by the solar wind across the magnetosphere and the voltage across a magnetospheric diameter in the undisturbed solar wind. This factor is $\sim$ 10–20%. Since the Y-component of the IMF is typically several nT, the penetrating field will thus be several tenths of a nT, which is difficult to detect in the presence of variable magnetospheric fields of order 10–100 nT. Statistical analysis of large data sets is thus required.

The first indication of this effect was found in near-Earth tail data by Fairfield (1979), and was subsequently detected at geosynchronous orbit by Cowley & Hughes (1983). Very detailed information for the former region has recently been presented by Kaymaz *et al.* (1994), who used IMP-8 tail data (at distances between 25 and 40R_E (Earth radii)) and simultaneous ISEE-3 interplanetary data, acquired over a four-year interval. The IMP-8 data were sorted into 2R_E boxes in

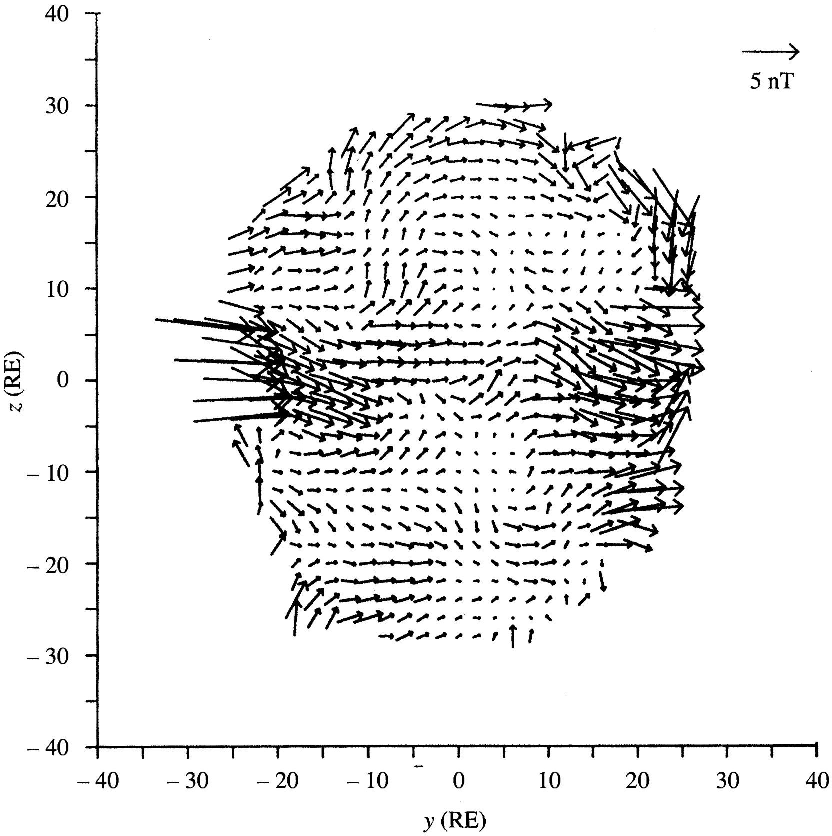

Figure 5. Magnetic perturbation field in the geomagnetic tail associated with the Y-component of the IMF. (From Kaymaz *et al.* (1994).)

the Y–Z plane, and also into four quadrants of simultaneous IMF direction in this plane; the latter quadrants were centred on the $\pm Y$ and $\pm Z$-directions. Figure 5 shows a cross-section through the tail in the Y–Z plane in which the average field in each box for the $-Y$ IMF quadrant has been subtracted from the average field in the same box for the $+Y$ quadrant; the resulting difference vectors can be thought of as twice the perturbation field associated with positive IMF B_y conditions. It can be seen that there is a net flux in the positive Y-direction which when averaged over the cross-section amounts to 14% of the simultaneous IMF B_y, in conformity with prediction. The distribution is highly non-uniform, however, and is largest near the central current sheet (especially on the flanks) for reasons which remain to be determined. Results obtained by differencing the IMF $\pm Z$ quadrant data (not shown here) similarly confirm the partial penetration of IMF B_z (13% on average).

4. Time-dependent convection in the magnetosphere

A fundamental prediction of Dungey's theory is that the magnitude of the flow should be modulated by the IMF, with the flow being strong when the IMF points south (negative Z-component), and weak when it points north. The first indications of this effect were obtained from studies of geomagnetic disturbance (Fairfield & Cahill 1966). Direct verification was first obtained by Reiff *et al.* (1981) who used ionospheric flow data from low-altitude spacecraft to measure the total voltage associated with the flow. This was found to be 50–100 kV for southward fields and 10–30 kV for northward fields, in conformity with expectation.

The question which follows is how and on what time-scale the flow reconfigures following changes in the IMF. A related issue concerns the time-dependent flow response to pulses of reconnection (such as FTEs) whether caused by IMF changes or not. Data from low-altitude spacecraft cannot be used for this purpose because they provide only few-minute snapshots in a given hemisphere every 90 min, while the flow generally varies much more rapidly than this. Rather, use must be made of ground-based radars which provide continuous flow monitoring at a given location, coordinated with simultaneous space observations, e.g. in the solar wind to monitor the IMF, at the magnetopause to look for the signatures of reconnection and FTEs, or in the tail to examine simultaneous substorm features.

Some of the first coordinated experiments were conducted in the mid-1980s using AMPTE-UKS and AMPTE-IRM to monitor the IMF, and the EISCAT UHF radar to monitor flow in the dayside ionosphere. A close correspondence was found between the flow and IMF B_z. When the field switched from north to south flow in the noon sector was found to be excited over the whole latitude range accessible to the radar experiment (71° to 75° magnetic latitude) 2 min after the field change was estimated to have reached the magnetopause (Etemadi *et al.* 1988). A 2-min delay is approximately the Alfvén propagation time from the subsolar magnetopause to the ionosphere. The flow excitation was observed to spread in local time away from noon with a phase speed of a few km s^{-1}, reaching the dawn–dusk meridian after $\sim$ 10 min. When the IMF turned from south to north a similarly prompt onset of flow decay was observed in the noon sector, with the flow dying away to small values on time-scales of $\sim$ 10–15 min, despite the continued existence of substantial open flux in the polar cap.

In a steady open magnetosphere driven by steady balanced reconnection at the dayside magnetopause and in the tail, the electric field on open field lines may be computed by mapping the interplanetary electric field along the magnetic field (assumed equipotential). The above results demonstrate that this is no longer true in the time-dependent case; the flow should instead be regarded as generated by changes in the open flux (production at the dayside or destruction in the tail) rather than the mere existence of open flux, such as is implicit in the theoretical work of Siscoe & Huang (1985). The important conclusion is that if reconnection were to be switched off at the dayside and in the tail (and all other coupling processes too) then flow would die away in the near-Earth system independent of how much open flux was present; the radar data and simple theory indicate a decay time of $\sim$ 10–15 min. During such intervals the length of the tail would simply increase at the solar wind speed.

Starting from such a configuration we may qualitatively discuss the response of the system to a pulse of reconnection either at the dayside or in the tail. This problem was discussed by Southwood (1987) and Freeman & Southwood (1988), and further developed by Cowley & Lockwood (1992). Figure 6, taken from the latter paper, shows the ionospheric flow response to an impulse of dayside reconnection; here we look down on the northern hemisphere with noon at the

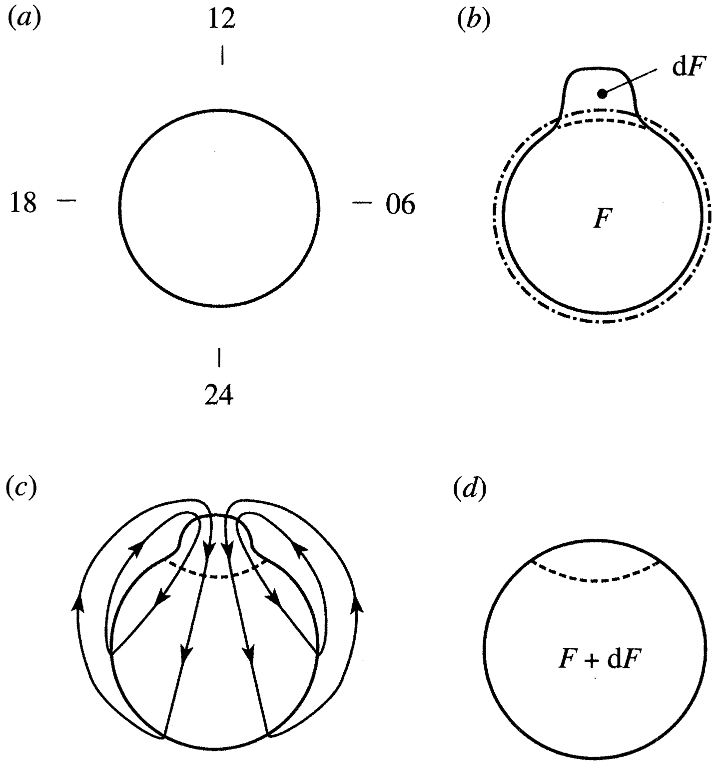

Figure 6. Excitation and decay of flow in the northern high-latitude ionosphere due to a pulse of dayside reconnection. (From Cowley & Lockwood (1992).)

top and dusk on the left. Sketch (*a*) shows the initial zero-flow equilibrium with open flux F. In sketch (*b*) a reconnection impulse has added open flux $\mathrm{d}F$ to the noon boundary; the equilibrium boundary for this amount of open flux is shown by the dot–dash line. In (*c*) a twin-vortex flow is excited which takes the perturbed system to the new equilibrium on a time-scale of $\sim$ 10–15 min; the flow starts near noon and then spreads over the whole polar cap as shown. After this the flow stops (until the next pulse of reconnection occurs), with the new open flux assimilated into the dayside open flux region (sketch (*d*)).

The flow shown in figure 6 corresponds to that expected for a purely southward IMF, but this may be readily extended, e.g. to include the effect of IMF B_y, to treat tail reconnection impulses, to discuss the flows for steady unbalanced dayside and nightside reconnection (the Siscoe–Huang problem), and, as a singular case, to steady state flow. The inclusion of B_y effects is important in discussing the flows associated with magnetopause FTEs since IMF B_y is commonly present. To date, however, there is only one published example of simultaneous flow pulses and auroral transients in the cusp ionosphere and FTEs at the magnetopause, obtained using EISCAT, ISEE-1 and ISEE-2 (Elphic *et al.* 1990). This is a matter which we intend to follow up using the extended EISCAT system, the Cutlass radar and the Cluster spacecraft.

The topic of nightside flow pulses and their relation to magnetotail activity and substorms is also one where major questions remain. EISCAT data analysed by

PHILOSOPHICAL TRANSACTIONS OF THE ROYAL SOCIETY A MATHEMATICAL, PHYSICAL & ENGINEERING SCIENCES

Williams *et al.* (1990) have shown that flows in the nightside auroral zone exhibit pulses which last for $\sim$ 5–10 min and recur on a few tens of minutes time-scales. Although these might be generated in radar data by a variety of effects, Morelli *et al.* (1994) have examined PACE radar and ground-based magnetic data and have shown that flow surges can be generated by impulsive electrojet activations associated with multiple-onset substorms. Simultaneous data from the EISCAT radar in the morning sector provided preliminary evidence that these surges extended several hours of local time in the nightside auroral zone. Although we may infer that these activations are associated with impulsive substorm depolarizations of the tail field, the nature of the physical process which leads to depolarization is a matter of considerable controversy (Cowley 1992). The principal contenders are pulsed reconnection in the near-Earth tail and sequential current sheet disruptions on closed field lines at the interface between the ring current and the plasma sheet. This is another matter which we intend to take up using data from the extended EISCAT system and Cluster.

References

Cowley, S. W. H. 1981 Magnetospheric asymmetries associated with the *Y* component of the IMF. *Planet. Space Sci.* **29**, 79–96.

Cowley, S. W. H. 1982 The causes of convection in the Earth's magnetosphere: a review of developments during the IMS. *Rev. Geophys. Space Phys.* **20**, 531–565.

Cowley, S. W. H. 1985 Magnetic reconnection. In *Solar system magnetic fields* (ed. E. R. Priest), pp. 121–155. Dordrecht, The Netherlands: Reidel.

Cowley, S. W. H. 1992 The role and location of magnetic reconnection in the geomagnetic tail during substorms. In *Substorms 1*, Proc. First International Conference on Substorms, ICS-1, ESA SP-335, pp. 401–404. Noordwijk, The Netherlands: ESA Publications.

Cowley, S. W. H. 1993 The magnetosphere and its interaction with the solar wind and with the ionosphere. In *The behaviour of systems in the space environment* (ed. R. N. DeWitt, D. Duston & A. K. Hyder), pp. 147–181. Dordrecht, The Netherlands: Kluwer.

Cowley, S. W. H & Hughes, W. J. 1983 Observation of an IMF sector effect in the *Y* magnetic field component at geostationary orbit. *Planet. Space Sci.* **31**, 73–90.

Cowley, S. W. H. & Lockwood, M. 1992 Excitation and decay of solar wind-driven flows in the magnetosphere–ionosphere system. *Ann. Geophysicae* **10**, 103–115.

Cowley, S. W. H., Morelli, J. P. & Lockwood, M. 1991 Dependence of convective flows and particle precipitation in the high latitude dayside ionosphere on the *X* and *Y* components of the interplanetary magnetic field. *J. geophys. Res.* **96**, 5557–5564.

Dungey, J. W. 1961 Interplanetary magnetic field and the auroral zones. *Phys. Rev. Lett.* **6**, 47–48.

Elphic, R. C., Lockwood, M., Cowley, S. W. H. & Sandholt, P. E. 1990 Flux transfer events at the magnetopause and in the ionosphere. *Geophys. Res. Lett.* **17**, 2241–2244.

Etemadi, A., Cowley, S. W. H., Lockwood, M., Bromage, B. J. I., Willis, D. M. & Luhr, H. 1988 The dependence of high-latitude dayside ionospheric flows on the north–south component of the IMF: a high time resolution correlation analysis using EISCAT 'Polar' and AMPTE-UKS and -IRM data. *Planet. Space Sci.* **36**, 471–498.

Fairfield, D. H. 1979 On the average configuration of the geomagnetic tail. *J. geophys. Res.* **84**, 1950–1958.

Fairfield, D. H. & Cahill, L. J. Jr. 1966 Transition region magnetic field and polar magnetic disturbances. *J. geophys. Res.* **71**, 155–163.

Freeman, M. P. & Southwood, D. J. 1988 The effect of magnetospheric erosion on mid- and high-latitude ionospheric flows. *Planet. Space Sci.* **36**, 509–522.

Fuselier, S. A., Klumpar, D. M. & Shelley, E. G. 1991 Ion reflection and transmission during reconnection at the Earth's subsolar magnetopause. *Geophys. Res. Lett.* **18**, 139–142.

Kaymaz, Z., Siscoe, G. L., Luhmann, J. G., Lepping, R. P. & Russell, C. T. 1994 IMF control of magnetotail magnetic field geometry: IMP-8 observations. *J. geophys. Res.*, **99**, 11 113–11 126.

Morelli, J. P., Bunting, R., Cowley, S. W. H. *et al.* 1994 Radar observations of auroral zone flows during a multiple-onset substorm. *Ann. Geophysicae*, submitted.

Reiff, P. H., Spiro, R. W. & Hill, T. W. 1981 Dependence of polar cap potential drop on interplanetary parameters. *J. geophys. Res.* **86** 7639–7648.

Russell, C. T. & Elphic, R. C. 1979 ISEE observations of flux transfer events at the dayside magnetopause. *Geophys. Res. Lett.* **6**, 33–36.

Siscoe, G. L. & Huang, T. S. 1985 Polar cap inflation and deflation. *J. geophys. Res.* bf 90, 543–547.

Smith, M. F. & Rodgers, D. J. 1991 Ion distributions at the dayside magnetopause. *J. geophys. Res.* **96**, 11617–11624.

Sonnerup, B. U. O., Paschmann, G., Papmastorakis, I., Sckopke, N., Haerendel, G., Bame, S. J., Asbridge, J. R., Gosling, J. T. & Russel, C. T. 1981 Evidence for magnetic reconnection at the Earth's magnetopause. *J. geophys. Res.* **86**, 10049–10067.

Southwood, D. J. 1987 The ionospheric signature of flux transfer events. *J. geophys. Res.* **92**, 3207–3213.

Williams, P. J. S., Virdi, T. S., Cowley, S. W. H. & Lester, M. 1990 Short-lived bursts of plasma velocity in the auroral zone. 1. Observational evidence from radar measurements. *J. Atmos. Terr. Phys.* **52**, 421–430.

PHILOSOPHICAL TRANSACTIONS OF THE ROYAL SOCIETY A MATHEMATICAL, PHYSICAL & ENGINEERING SCIENCES